International Journal of ChemTech Research
CODEN (USA): IJCRGG, ISSN: 0974-4290, ISSN(Online):2455-9555
Vol.11 No.10, pp 221-226, 2018

Numerical study of the global heat transfer coefficient in a shell-and-tube heat exchanger with a CFD software

Haner Andrés Escorcia[1], Gonzalo David Zapata[2], Guillermo Eliecer Valencia[3*]

[3]Efficient Energy Management Research Group, Universidad Del Atlántico km 7Antigua vía Puerto, Colombia

[1,2] Research Assistant in Mechanical Engineering/ Faculty of Engineering/Universidad Del Atlántico, Colombia.
[3]Assistant Professor in Mechanical Engineering Program/ Faculty of Engineering/ Universidad Del Atlántico, Colombia.

Abstract : In this study, the authors analyze the performance of a shell-and-tube heat exchanger with a CFD model done in ANSYS, and compare the results obtained from the simulation with the ones gotten form the laboratory bank. The study, done in parallel and crossflow in both laboratory and simulations, gave results well into the typified error margin for heat exchangers (close to 20%). The study's heat transfer coefficient was aprox. 12,8%-25,5% off compared to calculations done with experimental data. For the heat transfer rate, there was a divergence present because of the model used on the simulation. This divergence was more pronounced at high flows, increasing at higher temperatures and diminishing at lower temperatures.
Keywords : Shell and Tube Heat Exchanger, CFD Modelling, Software simulation.

1. Introduction

The Shell and Tube Heat Exchangers are well-known elements in the industry. It has been implemented a lot of time optimizing this type of heat exchangers, to reduce de operating costs and the environmental impact that they will be involved.

Perarasu & Arivazhagan compared the use of different nanofluids to optimize the heat transfer on helical-coil heat exchangers. Using concentrations of 0.1%, 0.2% and 0.3%, with Al_2O_3 improving the heat transfer rate between 13.6% and 28.9%, and TiO_2 improving that heat transfer rate between 6.51% and 17.59%[1,2]. Delaplace et al. used heat flux sensors to determine the heat transfer coefficient between the wall and the fluid of a heat exchanger with agitator, using those to check the renewal of the layers of fluid in contact with

DOI= http://dx.doi.org/10.20902/IJCTR.2018.111027

the wall, the performance compared with thermocouples and heat balance techniques[3]. Nassar & Mehrotra designed and built a heat transfer laboratory experiment to verify the heat transfer conditions in an agitated vessel. The apparatus could be operated under both static and flow conditions[4]. Khoshvaght-Aliabadi et al. did a study replacing water in an agitated serpentine heat exchanger, with concentration values of 0.1% and using Cu-water, Fe-water and Ag-water, evaluating the influence of volumetric flow in the ranges of 4-10 L/min and the agitator's rotating speed at 400, 800 and 1300 RPM[5].

Han et al. simulated a chevron-corrugated plates heat exchanger, to obtain a tridimensional plot of temperature, pressure and velocity of the fluid, comparing the simulation values with the experimental ones[6]. Fan et al. proposed a performance evaluation plot, using the ratios of heat transfer enhancement and friction factor increase as its variables[7]. Zhang et al. proposed an EEI (Energy Efficiency Index) to evaluate the energy efficiency of single-phase flow and heat transfer of plate heat exchangers[8]. Wang et al. used a 3D model of a chevron-corrugated plate heat exchanger and analyze the performance of the cold and hot fluid using the software ANSYS, easing the optimization process of the heat exchanger[9]. Andrzejczyk & Muszynski studied the influence of the continuous core-baffle geometry at mixed-convection heat transfer in shell- and-coil heat exchangers. With a power rang of 100W-1200W and mass flow rates in ranges of 0,01 kg/s-0,025 kg/s. This paper confirmed that new form of continuous baffle geometry can successfully enhance heat transfer, but using lower mass flow rates[10]. Eldeeb et al. did a review on available literature on the correlation for heat transfer and pressure drop calculations for two-phase flow in Plate Heat Exchangers[11]. Martin used the generalized Léveque equation to predict the performance of different chevron-type plate heat exchangers, using them to calculate heat transfer coefficients. This prediction is in good agreement with the experimental observations done in the literature[12]. Dvorak &Vit developed a simple CAE method for rapid design and optimization of the dimensions of plate heat exchangers. It proved that bigger heat exchangers provide higher effectiveness and lower pressure drop for the same flow rate, with the heat transfer surface being larger[13,14]. Zhang & Chen modelled and studied cross-corrugated triangular ducts to intensify the convective heat transfer coefficient on the surface of the membranes. The model was validated with heat transfer experiments and high speed hot wire anemometry technology[15].

Gertzos et al. used a CFD program to study the design of a water heater analyzed numerically, the results of the study determining the optimal position of the heater on a system using solar energy to supply heat to a water circuit[16]. Pal et al. used a flux simulator to understand the performance in a Shell and Tube Heat Exchanger (STHX) without and with baffles, comparing t them and finding that for $L/D_h<21$, Nusselt number is affected by a cross flow in the entrance of the exchanger, the presence of recirculation zones and leakage on the shell[17]. Ambekar et al. compared the heat transfer coefficient and the pressure drop on different configurations of baffles on a STHX, with simple baffle STHX getting a great global heat transfer coefficient, but suffering of high pressure drop, requiring more powerful and expensive pumps. The "flower" type of baffles were the most efficient, which had almost the same global heat transfer coefficient and has a lower pressure drop (almost 30% less than the simple baffle STHX)[18].

In this study, we analyzed the global heat transfer coefficient in the shell and tube heat exchanger obtained through experimentation, and doing a CFD modelling in ANSYS, comparing the obtained results. This analysis is done to study the viability to use the CFD modelling as a design tool for heat exchangers.

2. Materials and Methods

The following equations are determined by heat exchanger's design and can be found extensively in the bibliography[19,20].

Heat transfer rata is calculated by:

$$\dot{Q} = \frac{dQ}{dt} = U * A * \Delta T_{lm} \quad \textbf{(1)}$$

In that equation, U is the global heat transfer coefficient, A is the heat transfer area and ΔT_{lm} is the logarithmic mean temperature difference. The global heat transfer coefficient U for a specific heat exchanger is determined using the energy equation as-

$$U = \frac{1}{R_{theq}} \quad \textbf{(2)}$$

Where R_{theq} is the equivalent thermal resistance of the heat exchanger. The R_{theq} can be calculated using convective heat transfrer correlations, such as R_{cvi} (internal) and R_{cve} (external) along with the cylindrical conductive resistance R_{cd}. Ignoring the soiling resistance in the heat exchanger, assuming the pipe's diameter is very small and thermal conductivity is very high, then R_{cd} tends to zero. So the equation **(2)**is rewritten as-

$$R_{theq} = \frac{1}{h_i} + \frac{1}{h_e}, \textbf{(3)}$$

whereh_i and h_e are the convective coefficients.

To determine the internal convective coefficient, we calculate the Reynolds number:

$$Re = \frac{\rho V D_i}{\mu}, \qquad \textbf{(4)}$$

whereρ is the fluid's density, D_i is the internal diameter of the pipe, μ is the dynamic viscosity and V is the mean flow velocity, and is calculated as-

$$V = \frac{\dot{m}}{\rho A_f}, \textbf{(5)}$$

where$\dot{m}$ is water's masic flow and A_f is the internal flow area, obtained the expression as-

$$A_f = \frac{\pi N_t}{4N_p} {D_i}^2 \textbf{(6)}$$

Where N_t and N_p are the number of pipes and passes in the heat exchanger, respectively. The Nusselt number in a cylinder depends on the Reynold number's range, as the equation used to calculate Nusselt number varies accordingly.

$$Nu = 0{,}683 Re^{0{,}466} * Pr^{1/3} (40<\text{Re}>4000), \textbf{(7)}$$

$$Nu = 0{,}193 Re^{0{,}618} * Pr^{1/3} (4000<\text{Re}<40000), \textbf{(8)}$$

wherePr is Prandtl number. Finally, the convective coefficient is found with the next equation:

$$h_i = \frac{Nu * k_f}{D_i}, \textbf{(9)}$$

whereK_f is dependant of the mean temperature of the fluid.

To calculate the external convective coefficient, we use almost the same equations as the internal convective coefficient. Reynolds use the following formula:

$$Re = \frac{\rho V D_{eq}}{\mu}, \textbf{(10)}$$

where$V$ is calculated with equation **(5)**, but the flow area section $Af$is calculated as:

$$Af = B D_c \left(\frac{P_T - D_{eq}}{P_T}\right), \textbf{(11)}$$

where$B$ is the void between baffles, D_c is the tank diameter and the equivalent diameter for heat transfer is determined depending of the pipe's arrangement in the heat exchanger.

Model's description

In the CFD modelling, done in ANSYS software, the fluid is assumed stationary, incompressible and turbulent. Fluid's properties are assumed constant. The equations goberning the fluid are:

Continuity Equation

$$\frac{\partial u_i}{\partial x_i} = 0 \textbf{(12)}$$

Momentum Transport Equation

$$\rho \frac{\partial u_i}{\partial t} + \rho \frac{\partial u_j u_i}{\partial x_j} = -\frac{\partial p}{\partial x_i} + \frac{\partial}{\partial x_j}\left(\mu \frac{\partial u_i}{\partial x_j}\right) \textbf{(13)}$$

To model Reynolds stress (defined as $-\rho\, \partial\langle u_i' u_j'\rangle / \partial x_j$), we used Boussinesq hypothesis, so we have:

$$-\rho \partial\langle u_i' u_j'\rangle = \frac{2}{3} k\rho\delta_{ij} - \mu_t \left(\frac{\partial\langle u_i\rangle}{\partial x_j} + \frac{\partial\langle u_j\rangle}{x_i}\right) \textbf{(14)}$$

The energy equation is expressed as:

$$\frac{\partial T}{\partial t} + \frac{\partial(T\langle u_j\rangle)}{\partial x_j} = -\frac{\partial}{\partial x_j}\left(\left(\frac{\upsilon}{Pr} + \frac{\upsilon_t}{Pr_t}\right)\frac{\partial T}{\partial x_j}\right) \textbf{(15)}$$

Using the κ-ε turbulence model [21], the modelling equations are:

$$\frac{\partial k}{\partial t} + \frac{\partial\langle u_j\rangle k}{\partial x_j} = \frac{1}{\rho}\frac{\partial}{\partial x_j}\left[\left(\mu + \frac{\mu_t}{\sigma_k}\right)\frac{\partial k}{\partial x_j}\right] + \frac{P_k}{\rho} - \varepsilon, \textbf{(16)}$$

where, $P_k = \mu_t \left(\frac{\partial\langle u_i\rangle}{\partial x_j} + \frac{\partial\langle u_j\rangle}{\partial x_i}\right)\frac{\partial\langle u_i\rangle}{\partial x_j}$; and $\mu_t = C_\mu \rho \frac{k^2}{\varepsilon}$.

$$\frac{\partial \varepsilon}{\partial t} + \frac{\partial\langle u_j\rangle \varepsilon}{\partial x_j} = \frac{1}{\rho}\frac{\partial}{\partial x_j}\left[\left(\mu + \frac{\mu_t}{\sigma_\varepsilon}\right)\frac{\partial \varepsilon}{\partial x_j}\right] + C_{\varepsilon 1}\frac{\varepsilon}{k}\frac{P_k}{\rho} - C_{\varepsilon 2}\frac{\varepsilon^2}{k}, \textbf{(17)}$$

where C_μ=0,009; C_{s1}=1,44; C_{s2}=1,92; σ_k=1,0; σ_s=1,3.

3. Results and Discussion

For a shell and tube heat exchanger with initial conditions reflected in **Table I** and **Table II**, is showed the global heat transfer coefficient obtained for parallel flow and crossflow, we observed a higher heat transfer rate using the heat exchanger at crossflow, because of the ΔT present at the X-axis in the heat exchanger.

Table I. Constants used as initial values for hot fluid

N	0,000008 m^2/s
P	1000 kg/m^3

Table II. Constants used as initial values for cold fluid

T_{in}	293 K
ṁ	0,0125 m^3/s
ν	0,000008 m^2/s
ρ	1000 kg/m^3

For a heat exchanger in crossflow, it was observed that the global heat transfer coefficient does not vary significantly when was changed the flow into the shell as shown in Figure 1, but, when comparing the temperatures, the global heat transfer coefficient suffers a linear reduction, but this reduction is well into the accepted margin of error for heat exchangers of this type.

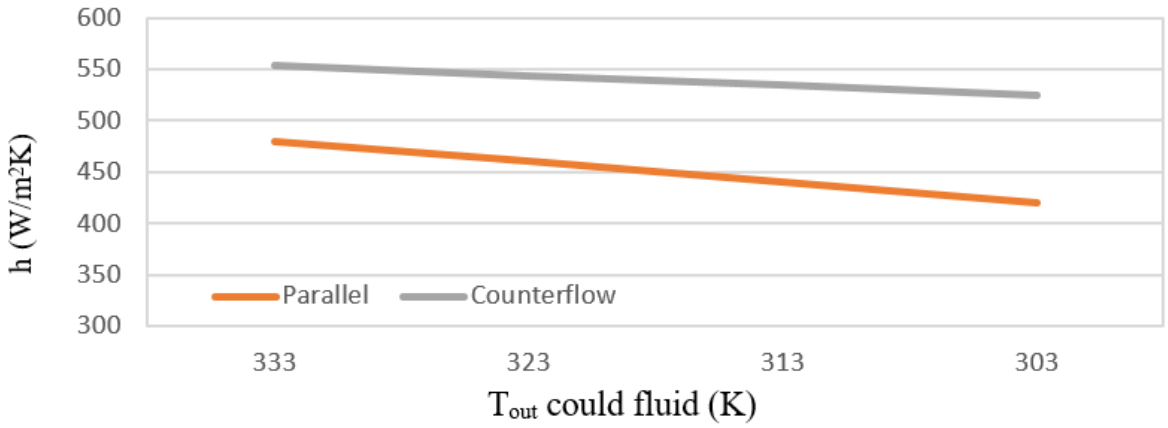

Figure 1. Heat Transfer Coefficient as function of the cold fluid outlet Temperature

When Comparing the heat transfer rate as shown in Figure 2, there is a significant divergence for flows higher than 0,021 m^3/s. This error could be a byproduct of the turbulence model used in the simulation (k-ε).

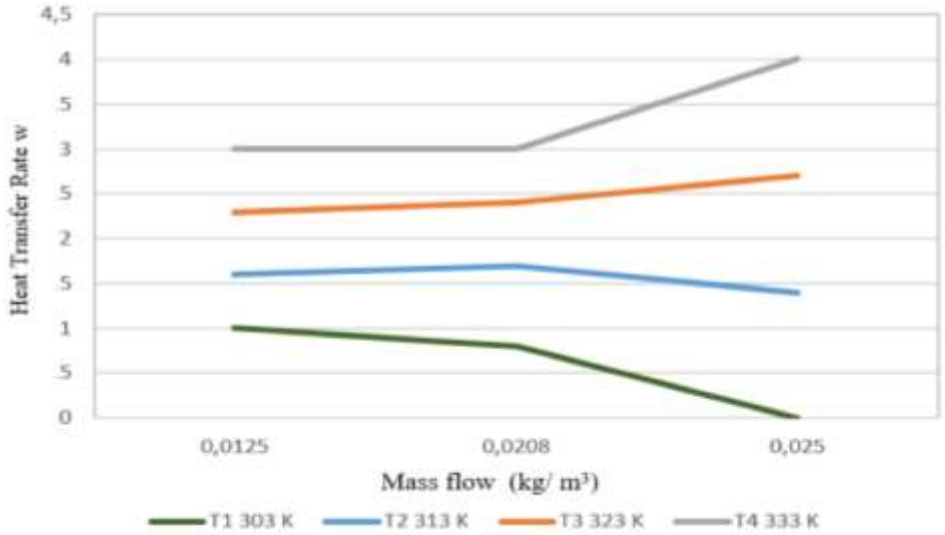

Figure II. Heat Transfer Rate as function of the mass Flow.

The heat transfer rate values with a flow of 0,025 m^3/s and a 303 K temperature presents a zero divergence, because the inlet and outlet temperatures tends to be equals, this meaning that the heat transfer rate is effectively tending to zero.

4 Conclusions

In this study, it was proved that the data given by the algorithm is approximately equal to the data obtained experimentally. The heat transfer coefficient presented a 12,8%-25,5% variation between the theoretical and experimental data. The simulation used a k-ε turbulence method, which can explain the tendency to zero present when evaluating at higher flows. The best homogenization of temperatures is present in a parallel flow, while the highest heat transfer rate was present in crossflow, allowing a ΔT higher than 4% total.

References

1. V. T. Perarasu, M. Arivazhagan, and P. Sivashanmugam, "Heat transfer of TiO2/water nanofluid in a coiled agitated vessel with propeller," *J. Hydrodyn.*, vol. 24, no. 6, pp. 942–950, Dec. 2012.
2. T. Perarasu, M. Arivazhagan, and P. Sivashanmugam, "Experimental and CFD heat transfer studies of

Al2O 3-water nanofluid in a coiled agitated vessel equipped with propeller," *Chinese J. Chem. Eng.*, vol. 21, no. 11, pp. 1232–1243, Nov. 2013.
3. G. Delaplace, J. F. Demeyre, R. Guérin, P. Debreyne, and J. C. Leuliet, "Determination of representative and instantaneous process side heat transfer coefficients in agitated vessel using heat flux sensors," *Chem. Eng. Process. Process Intensif.*, vol. 44, no. 9, pp. 993–998, Sep. 2005.
4. N. N. Nassar and A. K. Mehrotra, "Design of a laboratory experiment on heat transfer in an agitated vessel," *Educ. Chem. Eng.*, vol. 6, no. 3, pp. e83–e89, Aug. 2011.
5. M. Khoshvaght-Aliabadi, M. Nouri, O. Sartipzadeh, and M. Salami, "Performance of agitated serpentine heat exchanger using metallic nanofluids," *Chem. Eng. Res. Des.*, vol. 109, pp. 53–64, May 2016.
6. X. H. Han, L. Q. Cui, S. J. Chen, G. M. Chen, and Q. Wang, "A numerical and experimental study of chevron, corrugated-plate heat exchangers," *Int. Commun. Heat Mass Transf.*, vol. 37, no. 8, pp. 1008–1014, Oct. 2010.
7. J. F. Fan, W. K. Ding, J. F. Zhang, Y. L. He, and W. Q. Tao, "A performance evaluation plot of enhanced heat transfer techniques oriented for energy-saving," *Int. J. Heat Mass Transf.*, vol. 52, no. 1–2, pp. 33–44, Jan. 2009.
8. Y. Zhang *et al.*, "A quantitative energy efficiency evaluation and grading of plate heat exchangers," *Energy*, vol. 142, pp. 228–233, Jan. 2018.
9. Y.-N. Wang *et al.*, "A Study on 3D Numerical Model for Plate Heat Exchanger," *Procedia Eng.*, vol. 174, pp. 188–194, Jan. 2017.
10. R. Andrzejczyk and T. Muszynski, "An experimental investigation on the effect of new continuous core-baffle geometry on the mixed convection heat transfer in shell and coil heat exchanger," *Appl. Therm. Eng.*, vol. 136, pp. 237–251, May 2018.
11. R. Eldeeb, V. Aute, and R. Radermacher, "A survey of correlations for heat transfer and pressure drop for evaporation and condensation in plate heat exchangers," *International Journal of Refrigeration*, vol. 65. Elsevier, pp. 12–26, 01-May-2016.
12. H. Martin, "A theoretical approach to predict the performance of chevron-type plate heat exchangers," *Chem. Eng. Process. Process Intensif.*, vol. 35, no. 4, pp. 301–310, Jan. 1996.
13. V. Dvořák and T. Vít, "Evaluation of CAE Methods Used for Plate Heat Exchanger Design," in *Energy Procedia*, 2017, vol. 111, pp. 141–150.
14. V. Dvořák and T. Vít, "CAE methods for plate heat exchanger design," *Energy Procedia*, vol. 134, pp. 234–243, Oct. 2017.
15. L. Z. Zhang and Z. Y. Chen, "Convective heat transfer in cross-corrugated triangular ducts under uniform heat flux boundary conditions," *Int. J. Heat Mass Transf.*, vol. 54, no. 1–3, pp. 597–605, Jan. 2011.
16. K. P. Gertzos, Y. G. Caouris, and T. Panidis, "Optimal design and placement of serpentine heat exchangers for indirect heat withdrawal, inside flat plate integrated collector storage solar water heaters (ICSSWH)," *Renew. Energy*, vol. 35, no. 8, pp. 1741–1750, Aug. 2010.
17. E. Pal, I. Kumar, J. B. Joshi, and N. K. Maheshwari, "CFD simulations of shell-side flow in a shell-and-tube type heat exchanger with and without baffles," *Chem. Eng. Sci.*, vol. 143, pp. 314–340, Apr. 2016.
18. A. S. Ambekar, R. Sivakumar, N. Anantharaman, and M. Vivekenandan, "CFD simulation study of shell and tube heat exchangers with different baffle segment configurations," *Appl. Therm. Eng.*, vol. 108, pp. 999–1007, Sep. 2016.
19. Y. Cengel, *TRANSFERENCIA DE CALOR Y MASA*. 2007.
20. B. Zohuri and B. Zohuri, "Heat Exchangers," in *Physics of Cryogenics*, Elsevier, 2018, pp. 299–330.
21. W. Versteeg, H. K and Malalasekera, *An Introduction to Computational Fluid Dynamics*, vol. M. 2007.

*****